http://ansinet.com/itj

ITJ

ISSN 1812-5638

INFORMATION TECHNOLOGY JOURNAL

ANSInet
Asian Network for Scientific Information
308 Lasani Town, Sargodha Road, Faisalabad - Pakistan

Information Technology Journal 12 (23): 7709-7713, 2013
ISSN 1812-5638 / DOI: 10.3923/itj.2013.7709.7713

Compressed Sensing MRI with Walsh Transform-based Sparsity Basis

[1]Feng Zhen, [1]Guo He, [2]Wang Yu-Xin, [3]Xu Wen-Long, [4]Jiang Ming-Feng and [5]Liu Feng
[1]School of Software Technology, Dalian University of Technology, 116620, Dalian, China
[2]School of Computer Science and Technology, Dalian University of Technology, 116624, Dalian, China
[3]Department of Biomedical Engineering, China Jiliang University, 310018, Hangzhou, China
[4]School of Information Science and Technology, Zhejiang Sci-Tech University, 310018, Hangzhou, China
[5]School of Information Technology and Electrical Engineering, The University of Queensland, St Lucia, QLD 4072, Australia

Abstract: The choice of sparsity bases plays a crucial role to reconstruct high-quality MR images from heavily under-sampled k-space signals. Traditionally, the Wavelet transform and the Total Variation (TV) are used as the sparsity bases. In this study, a novel sparsity basis, based on a two-dimensional Walsh transform, is proposed to sparsify the MR image. The basic theory of the Walsh transform-based CS-MRI is explained and the proposed technique is validated with experiments. Three different types of MR images are used to test the proposed method performance in terms of reconstruction accuracy. The results show that the proposed Walsh transform-based sparsity basis is capable of reconstructing MRI images with a higher fidelity than the traditional Wavelet transform-based sparsity basis using a similar running time.

Key words: Compressed sensing, MRI, walsh transform, sparsity basis

INTRODUCTION

The development of a proper sparsity basis has been an important issue for the implementation of Compressed Sensing (CS). Given the precondition that the sensing matrix is incoherent with the sparsity basis, sparser representation requires fewer samples for a reliable CS reconstruction (Lustig *et al*., 2007).

For the CS application in Magnetic Resonance Imaging (MRI), there exist two categories of sparsity bases. The first category exploits the intensity distribution in the image domain, such as the Total Variation (TV) method (Huang *et al*., 2011) that identifies the global and local structures of the images and the K-SVD method (Aharon *et al*., 2006) that constructs an over-complete dictionary for sparse representation from image blocks. The second category transforms images into other coefficient matrices, such as discrete wavelet (Huang *et al*., 2011) and cosine transforms that concentrate most of the energy expressed with large coefficients.

The Walsh matrix is a typical square matrix (Fine, 1949), with sizes of a power of 2. The Walsh matrix has two properties: first, the entries are only +1 and -1 and second, the dot product of any two distinct rows (or columns) is zero, thus the rows (or columns) are orthogonal to each other. Because of the orthogonality, with the Walsh transform the spatial redundancy can be greatly reduced. In this way, energy concentrates in the largest coefficients of the transform matrix. Furthermore, the energy concentration property of the Walsh transform results in most of the coefficients being quite small, even zero. Previous literature has used the Walsh matrix as a sensing matrix to sparsify the reconstructed target (Li *et al*., 2012; Jiang *et al*., 2012). In the view of compressed sensing, it indicates that the coefficient matrix of the Walsh transform can act as a sparse representation of the MR image. In this work, we explore the possibilities of developing the Walsh transform as a novel sparsity basis for MR images in both theoretical and practical aspects.

THEORY

Suppose m is the target MR image, which is known to have a sparse representation in some transform Ψ. Φ_u is the sensing matrix, which transforms m into the k-space and then randomly acquires samples from the k-space; y is the acquired signal. Then, the CS-MRI problem is defined as:

$$\text{minimize: } \|\phi_u(m)-y\|_2+\lambda|\psi(m)|_1 \tag{1}$$

Corresponding Author: Guo He, School of Software Technology, Dalian University of Technology, 116620, Dalian, China

where, $\|\Phi_u(m)-y\|_2$ is the data fidelity regulation, $|\Psi(m)|_1$ is the data sparsity regulation, λ is the weighting parameter. In Eq. 1, the sparsity basis Ψ is expressed with a Walsh transform.

Given a one-dimensional signal f(x) with a size of $N = 2^n$, the Walsh transform and its inverse are defined as:

$$w(u)=\sum_{x=0}^{N-1} f(x)g(x,u) \tag{2}$$

$$f(u)=\sum_{u=0}^{N-1} w(u)h(x,u) \tag{3}$$

Here, g(x,u) is the Walsh transform kernel and h(x,u) is the inverse kernel function; g(x,u) and h(x,u) are identical to each other as:

$$g(x,u)=h(x,u)=\frac{1}{\sqrt{N}}(-1)\sum_{i=0}^{n-1} b_i(x)b_{n-1-i}(u) \tag{4}$$

where, $b_i(x)$ is the binary digit (0 or 1) at the i+1 position of the binary number x.

Similarly, given a two-dimensional signal f(x,y) with a size of M×N, where $M = 2^m$ and $N = 2^n$, the Walsh transform and its inverse are defined as:

$$w(u,v)=\sum_{x=0}^{M-1}\sum_{y=0}^{N-1} f(x,y)g(x,u,y,v) \tag{5}$$

$$f(u,v)=\sum_{u=0}^{M-1}\sum_{v=0}^{N-1} w(u,v)h(x,u,y,v) \tag{6}$$

The Walsh kernel function g (x,u,y,v) and its inverse h (x,u,y,v) are defined as:

$$g(x,u,y,v)=h(x,u,y,v)=\frac{1}{\sqrt{MN}}(-1)\sum_{i=0}^{m-1} b_i(x)b_{m-1-i}(u)+\sum_{j=0}^{n-1} b_j(y)b_{n-1-j}(v) \tag{7}$$

From Eq. 7, it can be found that the functions g (x, u, y, v) and h (x, u, y, v) are separable and can be expressed as:

$$g(x,u,y,v)=h(x,u,y,v)=g_1(x,u)g_2(y,v)=h_1(x,u)h_2(y,v) \tag{8}$$

$$g_1(x,u)=h_1(x,u)=$$

$$\frac{1}{\sqrt{M}}(-1)\sum_{i=0}^{m-1} b_i(x)b_{m-1-i}(u) \tag{9}$$

$$\frac{1}{\sqrt{N}}(-1)\sum_{i=0}^{n-1} b_i(y)b_{n-1-i}(v) \tag{10}$$

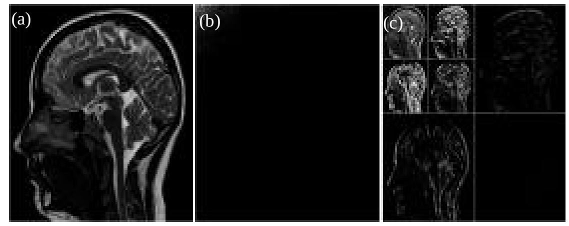

Fig. 1(a-c): Demo of sparsity bases, (a) Head image, (b) the Walsh transform coefficient matrix and (c) the wavelet transform coefficient matrix

Therefore, the two-dimensional Walsh transform can be implemented by successive one-dimensional Walsh transforms.

The Walsh transform has the energy concentration property; here, take a 4×4 matrix as an example, where all the entries are 1. The matrix f and its Walsh transform coefficient matrix W are computed as:

$$f=\begin{bmatrix}1 & 1 & 1 & 1\\ 1 & 1 & 1 & 1\\ 1 & 1 & 1 & 1\\ 1 & 1 & 1 & 1\end{bmatrix}$$

$$w=\begin{bmatrix}1 & 0 & 0 & 0\\ 0 & 0 & 0 & 0\\ 0 & 0 & 0 & 0\\ 0 & 0 & 0 & 0\end{bmatrix}$$

If the two-dimensional signal is smooth, then its Walsh transform coefficient matrix can be very sparse. This phenomena is also applicable for some kinds of MR images, such as the head image shown in Fig. 1a. To compute the Walsh transform coefficient matrix, the one-dimensional Walsh transform is performed on the head image column-by-column, then row-by-row. As shown in Fig. 1b, large coefficients concentrate on the top-left corner of the matrix, which is the sparse representation of the head image. For comparison, the Wavelet transform coefficient matrix is also illustrated in Fig. 1c.

Figure 2 compares the sparsity of the Walsh transform coefficient matrix and the Wavelet transform coefficient matrix of the given head image in Fig.1a. Figure 2a plots the sorted normalized coefficients of the Walsh and Wavelet transform matrices and Fig. 2b zooms in on the lower-left corner of the coordinate system. It can be observed that the Walsh transform coefficients decrease much faster than the Wavelet transform coefficients.

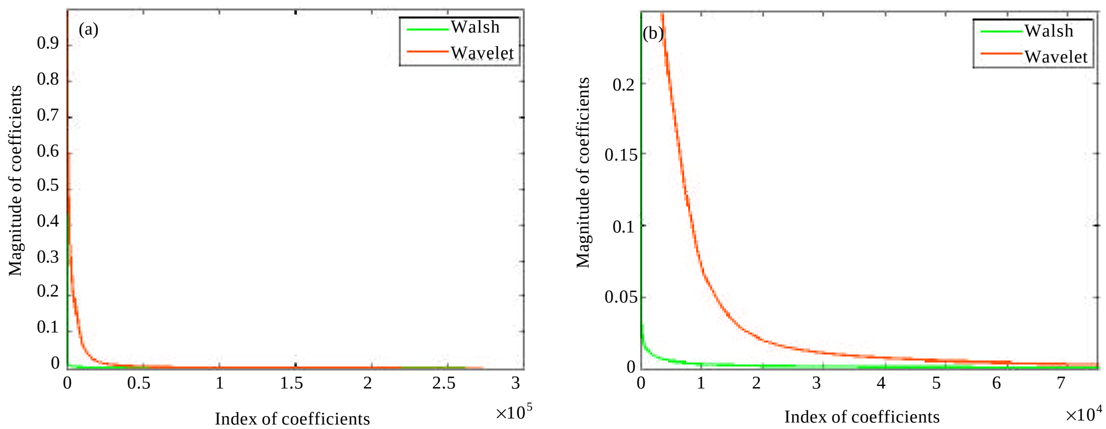

Fig. 2(a-b): Comparison of coefficient magnitudes with the Walsh and Wavelet transforms, (a) Global coefficients, (b) the lower-left zoomed-in coordinate system

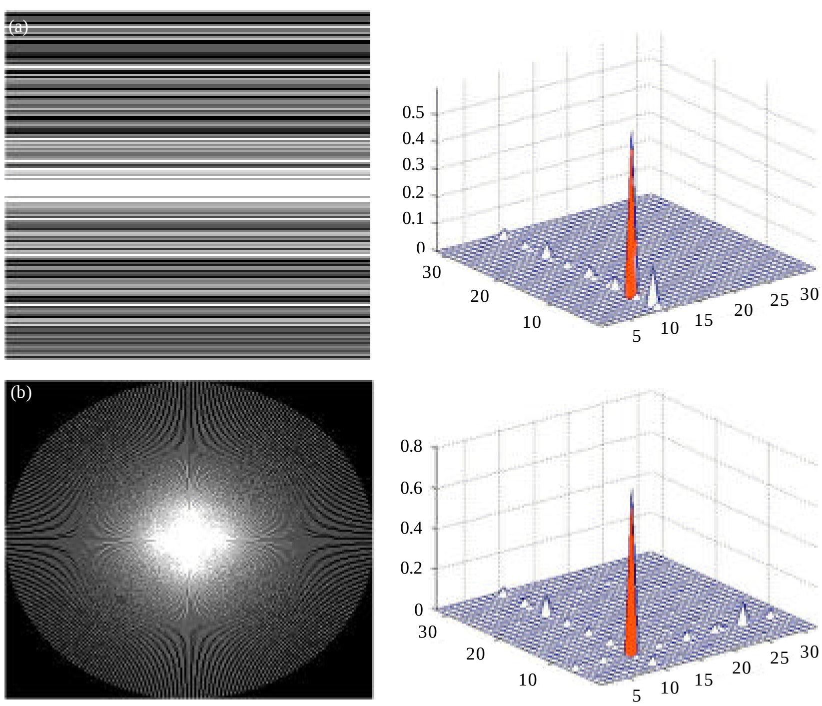

Fig. 3(a-b): Incoherence between under-sampled Fourier transform and the Walsh transform (a) for Cartesian sampling trajectory, (b) for radial sampling trajectory. The left column shows the under-sampling patterns, the right column shows the corresponding transform point spread function (TPSF) representations

The incoherence between the sensing matrix and the sparsity basis is a fundamental criterion for compressed sensing reconstruction. In CS-MRI, the sensing matrix is conventionally defined as an under-sampled Fourier transform. In this work, the Transform Point Spread Function (TPSF) was used to evaluate the incoherence between the under-sampled Fourier transform and the Walsh transform (Lustig *et al*., 2007). Figure 3 illustrates the TPSF results on two different sampling patterns. For the Cartesian sampling trajectory, a pulse is marked in red in the Walsh coefficient matrix and the result reveals that the artifacts only exist on the same row with the position of the pulse. For the radial sampling trajectory, the artifacts also only exist on the same row and column with the position of the pulse. Therefore, the artifacts are greatly suppressed on other positions and the incoherence is enhanced with the proposed Walsh transform-based sparsity basis.

With the demonstrated properties of sparsity and incoherence, we can now use the Walsh transform as a new sparsity basis for CS-MRI. Suppose m = f (x,y) is the two-dimensional MR image, then its sparse representation w(u,v) is defined as:

$$\psi(f(x,y)) = w(u,v) = \sum_{x=0}^{M-1}\sum_{y=0}^{N-1} f(x,y)\, g(x,u,y,v) b_i \tag{11}$$

MATERIALS AND METHODS

We have experimentally compared the Walsh-transform-based sparsity basis and the conventional Wavelet-transform-based sparsity basis and have tested two MRI datasets. As shown in Fig. 4, a head image and a breast image with sizes of 512×512 were acquired by a Siemens (Siemens Magnetom TIM Trio, Erlangen, Germany) 1.5T MRI system (CCAI, 2012). Cartesian trajectories and radial trajectories were considered when implementing the under-sampling of the k-space data. The reduction factors were set to be 4 and 6, respectively. The fast composite splitting algorithm (FCSA) was used to implement the CS-MRI reconstructions (Huang *et al*., 2011). Weights between the data fidelity and sparsity regulation were optimized from multiple trials, the iteration number was set to 50 in all cases. All the experiments were performed in the Matlab (Mathworks, Natick, United States) environment on a laptop with a 2.10 GHz Core i7 CPU, 6G memory and Windows 7 operating system. The reconstruction times were then recorded to measure the algorithm efficiencies.

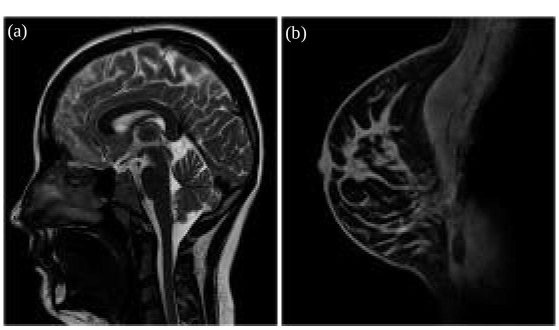

Fig. 4(a-b): MR datasets reconstructed with full k-space samples (512×512), (a) Head and (b) Breast

RESULTS

Table 1-4 and Fig. 5-6 compare the reconstruction results using both the Walsh transform and wavelet basis. The Signal-to-noise Ratio (SNR) was used to quantize the image qualities. In most cases, under the same experimental settings, the Walsh transform-based sparsity basis method achieved a higher SNR than that of the Wavelet transform-based sparsity basis. From the reconstruction results, it can also be found that, with the same reduction factor, the radial under-sampling pattern

Table 1: Reconstruction results of the head image under Cartesian trajectories

Reduction factor	Sparsity basis	SNR (dB)	Runtime (s)
4	Walsh	15.84	55.18
	Wavelet	15.72	64.25
6	Walsh	12.33	58.38
	Wavelet	12.48	63.90

Table 2: Reconstruction results of the head image under radial trajectories

Reduction factor	Sparsity basis	SNR (dB)	Runtime (s)
4	Walsh	26.01	53.83
	Wavelet	21.55	67.17
6	Walsh	20.69	53.72
	Wavelet	18.21	64.41

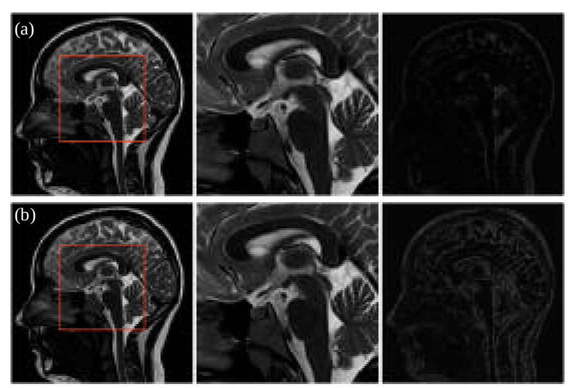

Fig. 5(a-b): CS reconstructed head image, (a) Row, using the Walsh transform-based method and (b) Row, using the Wavelet transform-based method. First column, reconstructed images. Second column, the zoom-in region of interest. Third column, error maps. In the implementation, it was based on a radial sampling pattern under a reduction factor of 4

Table 3: Reconstruction results of the breast image under Cartesian trajectories

Reduction Factor	Sparsity Basis	SNR (dB)	Runtime (s)
4	Walsh	21.31	56.23
	Wavelet	19.23	66.81
6	Walsh	15.71	56.73
	Wavelet	14.86	69.26

Table 4: Reconstruction results of the breast image under radial trajectories

Reduction factor	Sparsity basis	SNR (dB)	Runtime (s)
4	Walsh	32.64	52.23
	Wavelet	25.55	69.49
6	Walsh	28.17	56.03
	Wavelet	21.88	69.73

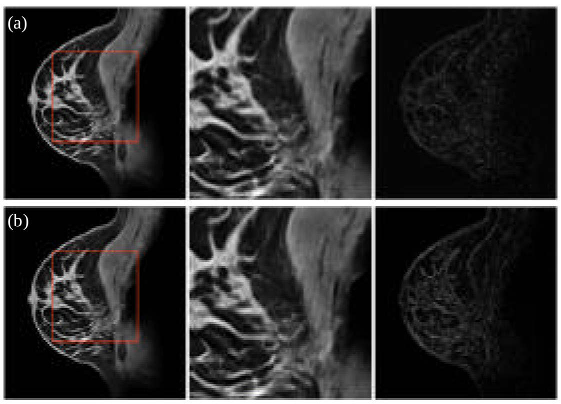

Fig. 6(a-b): CS reconstructed breast images, (a) Row, using the Walsh transform-based method and (b) Row, using the Wavelet transform-based method. First column, reconstructed images. Second column, the zoom-in region of interest. Third column, error maps. In the implementation, it was based on a radial sampling pattern and under a reduction factor of 6

was more effective than the Cartesian under-sampling pattern in reserving the dominant information of the k-space. The runtimes of the Walsh transform-based method were generally shorter than the Wavelet transform-based method, which results from the different execution times of the Walsh and Wavelet transforms. A typical Walsh transform on a 512×512 matrix took about 0.15 sec, while a typical level-1 Wavelet transform took about 0.27 sec.

CONCLUSION

In this study, for the CS-MRI reconstruction problem, a Walsh transform-based sparsity basis was proposed to sparsify the MR image. Experiments showed that the Walsh transform is well capable of sparsifying MR images and moreover, it is strongly incoherent with the under-sampling Fourier transform (sensing matrix). From the experimental results, it outperforms conventional sparsity bases, such as the wavelet transform. In our future work, we will exploit the artifact distribution characteristics and develop a blocked Walsh transform for the CS-MRI application.

REFERENCES

Aharon, M., M. Elad and A. Bruckstein, 2006. K-SVD: An algorithm for designing overcomplete dictionaries for sparse representation. IEEE Trans. Signal Process, 54: 4311-4322.

CCAI, 2012. Siemens open bore 1.5 Tesla MRI scanner. Cottage Centre for Advanced Imaging. http://www.cottageadvancedimaging.com/tabid/89/Default.aspx.

Fine, N.J., 1949. On the Walsh functions. Trans. Am. Math. Soc., 65: 372-414.

Huang, J., S. Zhang and D. Metaxas, 2011. Efficient MR image reconstruction for compressed MR imaging. Med. Image Anal., 15: 670-679.

Jiang, H., W. Deng and Z. Shen, 2012. Surveillance video processing using compressive sensing. Inverse Prob. Imaging, 6: 201-214.

Li, C., T. Sun, K.F. Kelly and Y. Zhang, 2012. A compressive sensing and unmixing scheme for hyperspectral data processing. IEEE Trans. Image Process., 21: 1200-1210.

Lustig, M., D. Donoho and J.M. Pauly, 2007. Sparse MRI: The application of compressed sensing for rapid MR imaging. Magnet. Resonance Med., 58: 1182-1195.